Summary of the Working Group on Few-Body Physics Workshop on Chiral Dynamics

R. Schiavilla

Jefferson Lab, Newport News, VA 23606
Department of Physics, Old Dominion University, Norfolk, VA 23529

U. van Kolck

Department of Physics, University of Arizona, Tucson, AZ 85721
RIKEN-BNL Research Center, Brookhaven National Laboratory, Upton, NY 11973
Kellogg Radiation Laboratory, California Institute of Technology, Pasadena, CA 91125

H.R. Weller

Triangle Universities Nuclear Laboratory and Duke University, Durham, NC 27708-0308

Systems of $A \geq 2$ nucleons are arguably the most interesting area of application of hadronic effective field theories (EFTs), because of a great confluence of factors absent in $A \leq 1$ systems: the theoretical challenge of combining a momentum expansion and a resummation to produce bound states, and the abundance of experimental data. $A \geq 2$ systems are also the newest playground for hadronic EFTs, even though Weinberg's seminal papers[1] date from almost ten years ago. The working group on few-body systems at Chiral Dynamics 2000 attests that this field is now viewed as part of mainstream Chiral Perturbation Theory (ChPT).

Few-nucleon systems provide, more generally, a unique testing ground for the simple, traditional picture of the nucleus as a system of interacting nucleons. The nucleon-nucleon (NN) interaction, as revealed by pp and np scattering experiments and the deuteron's properties, has a very rich structure. In light nuclear systems, with only a few degrees of freedom, it is possible to obtain accurate solutions for a wide variety of nuclear properties directly from realistic models of the NN interaction. Within this deceptively simple picture, we can test our understanding of nuclear structure and dynamics over a wide range of energy, from the few keV of astrophysical relevance to the MeV regime of nuclear spectra to the tens to hundreds of MeV measured in nuclear response experiments. Through the advances in computational techniques and facilities, the last few years have witnessed dramatic progress in the theory of light nuclei, as well as a variety of intriguing new experimental results. Important advances have occurred in studies of the spectra and structure of light nuclei, hadronic scattering, the response of light nuclei to external probes, and

electroweak reactions involving few-nucleon systems at very low energy.

By the Chiral Dynamics Workshop in Mainz in the summer of 1997, the first successes of Weinberg's power counting had been seen in the description of the $A = 2$ system [2], and in the derivation of $A = 3$ forces [3] and currents [4,5]. Nevertheless, some questions of consistency had also been raised: the roles of regularization, fine-tuning, and chiral-symmetry-breaking interactions [6] were unclear. A discussion of some of these issues can be found in a review talk at that conference [7].

Much progress has been made since then. The contributions to the working group, summarized here, reflect the current state of affairs in the rich interplay between theory–including the connection to the more conventional approach outlined above–and experiment.

1 EFT

Everything that is not forbidden by a symmetry is allowed. (This could be called the Weak Murphy Principle.) EFTs explore a separation of mass scales so as to order all allowed interactions according to the sizes of their contributions to observables. An expansion in Q/M results, where Q denotes the typical momentum (and light masses) and M the characteristic mass scale of the underlying theory. With such an ordering, many-nucleon forces and currents can be derived consistently, and from them observables can be calculated.

To each mass scale its own EFT. At present there is no well-established EFT for QCD at Q comparable to $M_{QCD} \sim m_\rho$. It is useful to consider separately the two cases $Q \lesssim m_\pi$ and $m_\pi \lesssim Q \lesssim m_\rho$. For simplicity, we limit ourselves here to two flavors.

1.1 $Q \lesssim m_\pi$

For momenta below the pion mass, all mesons (including the pion) and nucleon excitations can be integrated out, leaving only contact interactions among nucleons (N's), and gauge-invariant couplings between nucleons and photons. This EFT is not very interesting for $A = 1$, but in the $A \geq 2$ case it allows us to study many of the issues related to resummations, without having to worry about complicating long-range interactions.

Much of the progress since Mainz has been on this EFT. In fact, the power counting for this EFT was first advanced at the Mainz meeting [7], and developed shortly afterwards [8,9,10].

Scales

The underlying theory in this case is (a resummed version of) ChPT, and $M \sim m_\pi = 140$ MeV. Most dimensionful parameters in the EFT should be given by this scale; for example, the NN S-wave effective ranges $r_2 \sim 1/m_\pi$. For reasons not yet understood, however, a fine-tuning generates a second mass scale $\aleph \sim 1/a_2$, where a_2 stands for the NN scattering lengths, about 45 MeV in the $^3S_1$ and 10 MeV in the $^1S_0$ channels. The reason that this EFT is interesting is the power counting that says that: *(i)* $Q/\aleph$ terms have to be summed, generating a bound state where the typical momentum of the nucleons is $Q \sim \aleph$, or equivalently, where the binding energy $B_2 \sim \aleph^2/M$; and *(ii)* Q/M and $\aleph/M$ terms can be treated perturbatively, so the EFT is predictive, also for the bound state. It can be shown [10] that there no problems with regularization, although regularization in this non-perturbative context has a couple of subtleties. As it turns out, the leading-order NN interactions are simply of the form (neglecting spin and isospin factors) $C_0(N^\dagger N)^2$ with $C_0 \sim 4\pi/m_N\aleph$, while sub-leading interactions involve more and more derivatives. It can be also shown [10] that the EFT (which includes the deuteron d) is equivalent to the effective range expansion (ERE) for $A = 2$, but goes beyond ERE when $A \geq 3$ and/or photons are considered. Note that the ideas here are sufficiently general that the EFT can be used for other systems where the range of the interaction is smaller than the scattering length or, equivalently, the size of the bound state.

Few-body forces

Regarding $A \geq 3$ systems, the most important question is the relative size of many-nucleon forces, the most relevant for $A = 3$ being of the form $D_0(N^\dagger N)^3$.

Hans Hammer answered this question in this meeting [11]. He looked at Nd scattering in the S waves and showed the following. *(i)* In the $J = 3/2$ channel, where the Pauli Principle ensures only higher-derivative (thus high-order) $3N$ forces contribute, a low-energy theorem holds and the Nd phase shifts calculated with NN input alone are in excellent agreement with a phase shift analysis (PSA). The scattering length $a_3^{(3/2)}$ to sub-sub-leading order, for example, agrees with experiment to better than 1%; a comparison with results from Faddeev calculations employing the so-called "realistic" potentials can be found in Ref. [12]. *(ii)* In the $J = 1/2$ channel, the non-perturbative running of the renormalization group leads to an enhancement of the $3N$ force by the same fine-tuning that appeared in the $2N$ force, resulting in $D_0 \sim (4\pi)^2/m_N M^2 \aleph^2$. This interaction is then of leading order. Varying this one parameter, $A = 3$ doublet observables change correlatedly. (Such scaling had

in fact been observed in phenomenological models but left unexplained.) Now, if D_0 is fixed to the scattering length $a_3^{(1/2)}$, then the energy dependence of the doublet phase shifts is in agreement with a PSA, and the triton binding energy comes out $B_3 = 8.0$ MeV, less than 10% off. Hammer also showed an interesting application of the same ideas to Bose-Einstein condensates.

Fabrizio Gabbiani [13] considered higher waves in both channels. These waves are free of $3N$ forces to high order, and with parameters entirely fixed by NN data, good agreement was found with both a PSA and "realistic" potentials.

Currents

The interactions of photons with the $A = 2$ system have also been studied. Some of the results were described by Martin Savage in his review talk [14].

In the working group, Jiunn-Wei Chen [15] showed calculations of processes of astrophysical interest, for which little experimental information is available: $np \to d\gamma$, $\nu d \to l N N$ and $\bar{\nu} d \to \bar{l} N N$.

1.2 $Q \sim m_\pi \lesssim M_{QCD}$

In order to extend the energy regime of the theory, we need to include pions explicitly. The Lagrangian is then the same as in $A \leq 1$ ChPT, with the added multi-nucleon-field interactions. (Since $m_\Delta - m_N$ is not very different from m_π, it is wise to also include the Delta isobar as a propagating degree of freedom.) The crucial issue is how to compare the size of short-range (contact) terms and interactions from (long-range) pion exchange.

Scales

This issue is complicated by the fact that there are several scales floating around in this EFT. In the infrared, there is still $\aleph$; in the ultraviolet we have the mass of the degrees of freedom that have been integrated out, $M_{QCD} \sim m_\rho$. (I am assuming here that there is no symmetry or accident that generates extra light scales, besides those associated with chiral symmetry and $1/a_2$.) The introduction of the pion brings in two new mass scales, $f_\pi \simeq 93$ MeV and m_π. In NN irreducible diagrams, f_π appears with a 4π, and it is reasonable to include this combination in $M_{QCD} \sim 4\pi f_\pi$. In NN reducible diagrams, however, f_π appears with some other dimensionless number #. This combination sets the scale for pion effects in nuclei, and I will denote it $M_{nuc} \sim \# f_\pi$. Away from the chiral limit we have also m_π, which in the real world is numerically similar

4

to f_π. (The Delta brings in $m_\Delta - m_N$ but we will ignore this complication here.)

In order to power count [1], the simplest attitude is to assume $\# = O(1)$, to neglect the fine-tuning that makes $\aleph$ smaller than M_{nuc}, and to take $m_\pi \sim M_{nuc}$. This reduces the problem to two mass scales, M_{QCD} and $M_{nuc} \sim f_\pi \sim \aleph \sim m_\pi$. One thus should sum Q/M_{nuc} and m_π/M_{nuc} terms (no such terms appear if $A \leq 1$) while expanding in Q/M_{QCD} and m_π/M_{QCD} (as in ordinary ChPT). This includes summing up one-pion-exchange (OPE) ladders, and generating bound states at $Q \sim M_{nuc}$, that is, with binding energy $B_2 \sim M_{nuc}^2/M_{QCD} \ll M_{QCD}$. An estimate results, $B_2^{(3)} = O(10 \text{ MeV})$ in the $^3S_1$ channel, explaining the longstanding puzzle of why the deuteron is shallow compared to 1 GeV. This does *not* explain the fine-tuning that makes the deuteron even shallower, $B_2^{(3)} \sim 2.2$ MeV.

Alternatively [8], one may attempt to include the fine-tuning explicitly by counting powers of $\aleph$; one can also explore the fact that, as it appears in OPE, $\# \simeq 3$, and take the pion mass as small. That is, $\aleph \sim m_\pi \ll M_{nuc} \sim 3f_\pi$. If this is the case, one should sum $Q/\aleph$ terms while expanding in Q/M_{nuc}, $\aleph/M_{nuc}$ and m_π/M_{nuc}. A great simplification results, as the pion can be treated in perturbation theory and the pion ladder need not be resummed. On the other hand, convergence is slower; yet, in order to go beyond the pionless theory we need convergence in the region of Q bigger than m_π.

In the $A = 2$ system, Weinberg's power counting has been employed in the derivation of forces up to $O(Q^3)$ [2], a fit to data[2], the derivation of a hierarchy of isospin-violating interactions[16], and many other results, reviewed, for example, in Ref. [17]. One of the most interesting features is the appearance at $O(Q^2)$ and $O(Q^3)$ of two-pion-exchange (TPE) contributions whose long-distance part is completely determined by parameters that can be fitted in πN scattering. Recently this TPE has been seen in a new Nijmegen PSA[18], where it provides a better fit to the NN database than the long-range part of one-heavier-boson exchange. Such TPE could be used in phenomenological potentials.

In the working group, Mané Robilotta[19] presented some results on the effects of TPE on P and higher waves. In many of them the contribution of TPE is significant, and in all cases it goes in the direction of the phase shifts from PSAs. More extensive results on the NN system were presented by Ulf Meißner[20]. He introduced a potential in principle equivalent to the one in Ref. [2], but with some technical differences. First, for the sake of few-body calculations, a unitary transformation was made to remove energy dependence. Second, loops in the potential and in the iteration of the potential were regularized by different procedures. Third, TPE parameters were determined from the ChPT analyses of πN scattering that have appeared recently. The result

is a simpler and consequently better fit than in Ref. [2]. It is conceivable that the $O(Q^4)$ potential will achieve the precision of "realistic" phenomenological potentials.

Not all is rosy, however. Refs. [6,8] have pointed out some apparent inconsistencies with Weinberg's power counting. In the $^1S_0$ channel, renormalization of the pion ladder seems to require a counterterm proportional to m_π^2, which poses difficulties for an m_π/M_{QCD} expansion with non-perturbative pions. In the $^3S_1$ channel, a perturbative argument implies that thrice-iterated OPE needs a Q^2 counterterm, which could invalidate a Q/M_{QCD} expansion. These issues have not yet been resolved.

In the working group, Tom Mehen[21] presented results that show that Kaplan et al's power counting is also problematic in the momentum region where pions should be included explicitly, that is, $Q \sim m_\pi$. In striking contrast to Meißner's results, Mehen's calculated $^3S_1$ and ^3P_i phases do not show convergence at $Q \sim m_\pi$, and in next-to-next-to-leading order provide very poor fits of the Nijmegen PSA. This suggests a failure of the Q/M_{nuc} expansion.

Few-body forces

Few-nucleon systems have been studied within both power countings.

In the case of perturbative pions, Harald Grießhammer[22] showed that the results for Nd scattering are very similar to the pionless theory. He calculated the $J = 3/2$ S-wave phase shift above break-up, even beyond relative momentum m_π. Pionless and perturbative-pion EFTs show little difference in sub-leading order, and both agree well with "realistic"-potential calculations and (at higher energies) with a pd PSA.

In the case of non-perturbative pions, if they have naive sizes, $3N$ forces appear[3] at $O(Q^2)$ with explicit Deltas, and at $O(Q^3)$ if Deltas are integrated out, while AN, $A \geq 4$ forces appear at higher orders. This smallness of multi-nucleon forces is in agreement with potential-model phenomenology. To $O(Q^3)$, there are three types of $3N$ forces[3]. *(i)* There are contact forces as in the pionless theory. One outstanding question is whether the enhancement discovered by Hammer will persist at higher momenta. This is not obvious because the $3N$ force in the pionless theory subsumes diagrams which are iterations of the leading $2N$ force in the pionful theory. *(ii)* There are TPE forces, which are equivalent to the Tucson-Melbourne-Brazil force, once the latter is corrected in a small term. The parameters in this force are the same ones that are fixed in πN scattering and appear in the TPE NN force. Clearly, this a consistency that conventional approaches still lack. *(iii)* There are forces of mixed short- and OPE-range, with so-far unknown parameters.

Meißner[20] showed results for the $A = 3, 4$ systems calculated in $O(Q^2)$, where there are no $3N$ parameters. Nd observables come out very well, including the analyzing power A_y, which has been a problem for "realistic" potentials (even when the Tucson-Melbourne force is added). Binding energies of the triton and the alpha particle turn out to be comparable to those of "realistic" potentials (without added $3N$ forces). However, these binding energies change by about 15% when the cutoff varies by 10%. Because of the small cutoff range, it is not yet possible to confirm the non-enhancement of the short-range $3N$ force.

Chris Hanhart[23] discussed the relation between p-wave pion production in NN collisions and the mixed-ranged $3N$ force. Because it involves momenta $p \sim \sqrt{m_N m_\pi}$, $NN \to NN\pi$ requires a new power counting, which he formulated as an extension of Weinberg's counting. Working in sub-leading order in the expansion, he displayed two observables: *(i)* a polarized cross section that to this order can be predicted, where he found reasonable convergence and agreement with data; *(ii)* the amplitude for an S to S NN transition that is affected by (a certain combination of) the same parameters that affect the mixed-ranged $3N$ force, where he found that natural values can fit the data well. Bira van Kolck[24] showed that, in a hybrid calculation (where the NN potential was taken as the Argonne $v18$ potential), the same natural values for the parameters give a non-negligible contribution to A_y. Although the actual size of these terms can only be ascertained after the parameters are better determined and after a fully consistent EFT calculation is performed, this result shows that a solution of the so-called A_y puzzle is likely at $O(Q^3)$, but cannot yet be guaranteed from the promising results at $O(Q^2)$.

Currents

The successes in processes with external probes carry over to the pionful theory.

Grießhammer[22] showed results for $\gamma d \to \gamma d$ at 49 and 69 MeV in the perturbative-pion theory to next-to-leading order. He found good convergence and good agreement (as expected, better at 49 MeV) with existing data.

Silas Beane[25] considered the same reaction in the non-perturbative-pion theory to $O(Q^3)$. Convergence and good agreement (for well-understood reasons, better at 69 MeV) with the same data was also observed. He also reviewed calculations for $\gamma^{(*)} d \to \pi^0 d$, including a prediction for the photoproduction cross section at threshold that differed by a factor of 2 from conventional calculations, and was subsequently corroborated by experiment.

Kuniharu Kubodera[26] reviewed other reactions involving photons in the non-perturbative-pion theory. In particular, he showed results for spin observ-

ables in $np \to d\gamma$ at thermal neutron energies that are similar to those obtained in the perturbative-pion theory and agree with existing experiment.

1.3 To be done...

Clearly, $A \geq 2$ systems provide great challenges for EFT, and a lot remains to be understood and calculated.

Because of its simplicity, the pionless EFT affords high-order calculations. Although limited to small energies, very high accuracy can be obtained. This includes processes of astrophysical relevance, as discussed by Chen. The recent understanding of the $A = 3$ system, as described by Hammer, opens the door to a new set of reactions. For example, $nd \to \gamma t$ should be doable, and is one of the rare cases that potential models have trouble reproducing precisely [27].

As pointed out by Hammer, from the point of view of implications to light-nuclei structure, the next issues to resolve relate to $A = 4$. Because of the Pauli principle, the last possible leading-order force is of the type $E_0(N^\dagger N)^4$. We need to find out if this $4N$ force is sufficiently enhanced by its running at low energies as to be leading order, as it happens with the $3N$ force. If so, the force can be fitted to a single $4N$ observable, and then the EFT could be used to make leading-order, parameter-free predictions for everything else in its regime of validity. Hammer's results suggest the triton falls into this regime, but success with the alpha particle will be a better indicator of the usefulness of this EFT, since the alpha particle is more representative of typical nuclei.

Eventually, we want to better understand the pionful theory, which makes closer contact with modern phenomenological approaches. Currently we have a power counting that works well despite apparent inconsistencies, and a fully consistent power counting that does not seem to work. Mehen has shown that there is good indication that m_π^2 terms *can* be treated in perturbation theory. Beane has been working on the *non*-perturbative renormalization of the singular OPE potential, and his preliminary results are that a single momentum-independent counterterm suffices.

This suggests that the correct power counting will imply a summation of Q/M_{nuc} terms as in Weinberg's power counting, but an expansion in m_π/M_{nuc} as in Kaplan et al's counting. For $A = 2$ in leading order, one would have non-derivative contact interactions and the $m_\pi \to 0$ piece of OPE iterated to all orders. From existing results, one can be confident that this would generate an unambiguous chiral expansion and good fits. The rationale for this new power counting is clear in the chiral limit, but less so in the real world where m_π and M_{nuc} are comparable.

Processes involving external probes might provide extra information about

the best way to power count. For example, Grießhammer is studying $\gamma^{(*)}d \to \pi^0 d$ in the perturbative-pion theory, and this might provide an independent test of convergence. Processes like these are also useful to constrain neutron parameters. Beane is working on $\gamma d \to \gamma d$ to $O(Q^4)$ in the non-perturbative-pion theory in order to determine the neutron polarizabilities.

We can look forward to much more progress...

... *before Jülich.*

2 The conventional approach

In the *conventional* approach, nuclei are regarded as systems of nucleons interacting among themselves via two- and three-body interactions, and with external electro-weak probes via one- and many-body currents. The usefulness of such a picture lies in its conceptual simplicity. While this description of nuclei is not new, the ability to perform reliable calculations within such a model is fairly new, however. Calculations with local interactions began in the late sixties [28], but convergence of the partial-wave expansion was convincingly demonstrated only in the mid eighties [29]. Four-nucleon ground-state calculations followed in the early nineties [30]. The pace of progress has accelerated in the past decade, culminating in the numerically exact calculations [31] of low-lying states of nuclei with A=8–10. Also new is the connection, through chiral perturbation theory (ChPT), of such a picture within QCD [1]. Important conclusions of ChPT, in particular the relative smallness of many-body forces, have been confirmed by the phenomenological models.

If progress involved only nuclear ground states, the picture would be interesting but of limited utility. However, important progress has been made in the scattering regime as well. Realistic calculations of three-nucleon (nd and pd) scattering have been performed with Faddeev [32] and correlated-hyperspherical-harmonics [33] (CHH) techniques. Comparisons are available with a wide range of experimental observables, including total cross sections, vector and tensor analyzing powers, spin transfer coefficients, and scattering into specific final-state configurations. The overall agreement between theory and experiment is quite good, as many observables are well-reproduced in the calculations. Nevertheless, some discrepancies remain still unresolved. In particular, the difference between calculated and experimental results on the polarization observable A_y are quite puzzling, possibly pointing to the need for improved models of the three-nucleon interaction and the inclusion of relativistic effects.

Significant progress has also been made in calculating low-energy electroweak reactions with realistic strong interactions and electroweak couplings. Reactions such as ^{1}H(p,e$^+\nu_e$)^{2}H, ^{2}H(p,γ)^{3}He, ^{2}H(d,γ)^{4}He, and ^{3}He(p,$^+\nu_e$)^{4}He

have great astrophysical interest, as well as being important tests of our understanding of few-body reactions. They are sensitive both to ground- and scattering-state wave functions and the electroweak current operators. Several methods have been used successfully in studying these low-energy capture reactions, including Faddeev [34,35], CHH [36,37], and quantum Monte Carlo techniques [38].

The construction of realistic models of the nuclear current have proven essential to success in this area. Two-body currents associated with the NN interaction, particularly those associated with pion exchange, are crucial both on theoretical grounds, in order to satisfy current conservation, and phenomenological grounds, as they provide a much improved description of the properties of light nuclei. The Faddeev [34] and CHH calculations [36,37] of the ^{2}H(p,γ)^{3}He and ^{2}H(n,γ)^{3}H cross sections are in good agreement with experimental values. The four-body capture reactions are particularly sensitive to the detailed model of the interactions and currents, as their cross sections vanish in the limit of no tensor force and no two-body currents. Discrepancies exist between variational estimates of the ^{2}H(d,γ)^{4}He [39] and ^{3}He(n,γ)^{4}He [38] cross sections and the corresponding experimental values, and it is not yet clear whether these discrepancies are to be ascribed to deficiencies in the variational wave function or to the model of two-body current operator (or both).

Electron scattering experiments provide further crucial tests of our understanding, in particular probing the electromagnetic current operator at higher values of the momentum transfer. Again, ground-state properties are well reproduced within this picture. The framework presented in this article has been shown to provide, at low and moderate values of the momentum transfer, a satisfactory description of the deuteron structure functions and threshold disintegration, the elastic and transition form factors of the hydrogen and helium isotopes and ^{6}Li nucleus–for a review, see Ref. [40]. The only ground-state observables for which small but definite discrepancies exist between theory and experiment are the quadrupole moment of the deuteron, and the ^{3}He magnetic form factor in the region of the first diffraction minimum. The discrepancy in the deuteron quadrupole moment is significant, it is a challenge to obtain precise agreement with all the deuteron data in either a relativistic or non-relativistic model.

The conventional approach–interactions and currents and, in particular, the role played by their pion-exchange components–were critically reviewed by J. Carlson, V.R. Pandharipande, D.O. Riska, and R. Schiavilla. These contributions are now summarized below.

Realistic models of two-nucleon interactions

Realistic two-nucleon interactions consist of a long-range part due to one-pion exchange (OPE), and a short-range part either modeled by one-boson exchange (OBE), as in the CD-Bonn [41] and Nijmegen I [42] models, or parametrized in terms of suitable functions of two-pion range or shorter, as in the Argonne v_{18} (AV18) [43], Reid 93, and Nijmegen II [42] models. The short-range part is then constrained to reproduce accurately the NN scattering data up to 350 MeV lab energies. While these interactions are phase-equivalent —they all fit the Nijmegen data-base with a χ^2 per datum close to one— they differ in the treatment of non-localities. The AV18 and some of the Nijmegen models (Reid 93 and Nijmegen II) are local in LSJ channels, while the CD-Bonn and Nijmegen I have strong non-localities. In particular, the CD-Bonn has a non-local OPE interaction. However, it has been known for some time [44], and recently re-emphasized by Forest [45], that the local and non-local OPE interactions are related to each other via a unitary transformation. Therefore, the differences between local and non-local OPE cannot be of any consequence for the prediction of observables, such as binding energies or electromagnetic form factors, provided, of course, that three-body interactions and/or two-body currents generated by the unitary transformation are also included [46]. This fact has been demonstrated [47] in a calculation of the deuteron structure function $A(q)$ and tensor observable $T_{20}(q)$, based on the local AV18 and non-local CD-Bonn models and associated (unitarily consistent) electromagnetic currents. The remaining small differences between the calculated $A(q)$ and $T_{20}(q)$ are due to the additional short-range non-localities present in the CD-Bonn. The upshot is that, provided that consistent calculations–in the sense above–are performed, present "realistic" interactions will lead to very similar predictions for nuclear observables, at least to the extent that these are influenced predominantly by the OPE component.

One-pion exchange and the structure of nuclei

The long-range OPE and short-range repulsion in the NN interaction induce, among the nucleons in a nucleus, strong spatial, spin-isospin correlations, which influence the structure of the ground- and excited-state wave functions [48]. Several nuclear properties reflect these features of the underlying interaction. For example, the two-nucleon density distributions in states with pair spin S=1 and isospin T=0 are very small at small internucleon separations, and exhibit strong anisotropies depending on the spin projection S_z. Nucleon momentum distributions and, more generally, spectral functions have high momentum p and energy E components extending over a wide range of p and E values,

which are produced by short-range and tensor correlations. Finally, these correlations also affect the distribution of strength in response functions, which characterize the response of the nucleus to a spin-isospin disturbance injecting momentum and energy in the system. For a review of these issues, see again Ref.[40].

The short-range structures present in the $T, S = 0, 1$ two-nucleon densities are particularly interesting[48]. The interaction is very repulsive for $r < 0.5$ fm regardless of the S_z value. However, for distances $\simeq 1$ fm, it is very attractive when the two nucleons, in state $S_z=0$, are confined in the xy-plane, and very repulsive when they are along the z-axis; in contrast, when the two nucleons are in state $S_z=1$, the interaction is repulsive (but not as repulsive as for $S_z=0$) when the two nucleons are in the xy-plane, and very attractive when they are located along the z-axis. The energy difference between the two spatial configurations with $S_z=0$ is found to be very large, a few hundreds of MeV, in all realistic NN interactions. As a result, two-nucleon densities in nuclei are strongly anisotropic.

The deuteron is a particularly interesting case, since for it the two-nucleon density is simply related to the single-nucleon density —the reason being that the relative distance between the two nucleons is twice the distance between each of the nucleons and the center of mass. The single-nucleon equidensity surfaces have toroidal or dumbbell-like shapes[48], depending on whether the deuteron is in a state with $J_z=0$ or $J_z=1$. The torus-like structure, at a density of 0.24 fm^{-3} corresponding to 2/3 the maximum density, has a diameter of 1.4 fm and a thickness of 0.9 fm. Of course, in the absence of the tensor interaction, the deuteron D state would vanish, and the equidensity surfaces would consist of concentric spheres for any value of the density. Note that other realistic interaction models produce very similar results.

The presence of these short-range structures, predicted by conventional interaction models, has been recently confirmed experimentally by measurements of the $T_{20}(q)$ observable in the deuteron[49]. In particular, their dimensions (the diameter of the torus, for example) as inferred from the data, are in agreement with the values above, after relatively small corrections due to relativistic effects and contributions from two-body charge operators are folded into the analysis of the data. The experimental evidence thus suggests that realistic interaction models predict deuteron wave functions, which seem to be valid down to internucleon separations of $\simeq 0.7$ fm. It also indicates the crucial role played by the D state in the deuteron structure.

As already mentioned above, in nuclei the calculated $T, S = 0, 1$ two-nucleon densities with $S_z = \pm 1$ and 0 display short-range structures which are remarkably similar to those found in the deuteron[48], suggesting that these are

12

universal features. That the neutron-proton relative wave function in a nucleus is similar, at small separations, to that in the deuteron had been conjectured, quite some time ago, by Levinger and Bethe Lev50. Tensor correlations, i.e. D-state components induced by the tensor interaction, strongly influence also two-cluster distributions[48], such as $\vec{d}\vec{p}$ in ^{3}He or $\vec{d}\vec{d}$ in ^{4}He. These distributions exhibit spin-dependent spatial anisotropies, which can be understood in terms of the underlying toroidal or dumbbell structures of the polarized deuteron. In particular, the density is enhanced in the direction corresponding to the most efficient or compact placement of the deuteron relative to the remaining cluster, and it is reduced in those directions that would lead to very extended structures. These structures are expected to produce cross section asymmetries in exclusive experiments of the type $(e, e'\vec{d})$, and the experimental confirmation of their presence, as of yet still lacking, would be most interesting.

Three-nucleon interactions

Local and non-local realistic two-nucleon interactions underbind nuclei, and fail to reproduce quantitatively nd and pd scattering data in numerically exact calculations. They also overbind[51] symmetric nuclear matter and overestimate, typically by a factor of two, its equilibrium density. Thus the nuclear Hamiltonian needs to be supplemented at least by a three-nucleon (NNN) interaction, if it to has to provide a quantitative description of binding and reactions.

All current models of three-nucleon interactions incorporate a two-pion-exchange term, arising from the intermediate excitation of a Δ resonance, known as the Fujita-Miyazawa term[52]. This term alone, however, is found to be too attractive. Of course, other effects enter as well. Several groups have performed calculations with explicit Δ-isobar degrees of freedom in the nuclear wave function[53,54], and generally have found that the attraction from the long range two-pion-exchange NNN is canceled by dispersive effects at shorter distances and hence there is little net attraction.

Within a nucleons-only picture, several explicit models of the NNN interactions have been proposed. One of them was put forward by the Tucson-Melbourne group[55], a three-nucleon interaction based upon a pion-nucleon scattering amplitude derived using PCAC, current algebra, and phenomenological input. This interaction contains the long-range 2π-NNN, but also has additional structure at shorter distances. More recent versions contain ρ-exchange as well as pion-range forces between the three-nucleons, with the π-ρ components of the interaction being repulsive in light nuclei. These models have been used in many different calculations, and the short-distance πNN

cut-off can be adjusted to reproduce the triton binding energy. The cut-off dependence of the results is significantly smaller in models which include ρ exchange.

Another model has been derived by the Brazilian group[56], by using tree-level diagrams of effective Lagrangians which are approximately invariant under chiral and gauge transformations. After proper adjustments of the parameters, the resulting force gives similar results in the trinucleon bound states as the Tucson-Melbourne model.

A somewhat different approach has been taken by the Urbana-Argonne group[57]. Given the uncertainties in the three-nucleon interaction at distances shorter than pion-exchange, the interaction is taken as the sum of the 2π-NNN plus a central term, of two-pion range on each of two legs. This latter term is meant to simulate the dispersive effects which are required when integrating out Δ degrees of freedom. These terms are repulsive, and are taken, in this model, to be independent of spin and isospin.

The strengths of the two-π and central NNN interactions are adjusted to reproduce the triton binding energy, and to provide additional repulsion in hypernetted chain variational calculations of nuclear matter near equilibrium density. The resulting Hamiltonian, denoted as the AV18/UIX model[57], predicts reasonably well the low-lying energy spectra of systems with $A \leq 8$ nucleons in "exact"Green's function Monte Carlo calculations[58]. The experimental binding energies of the α particle is very well reproduced, while those of the A=6–8 systems are underpredicted by a few percent. This underbinding becomes (relatively) more and more severe as the neutron-proton asymmetry increases. An additional failure of the AV18/IX Hamiltonian is the underprediction of spin-orbit splittings in the excitation spectra of these light systems. These failures have in fact led to the development of new three-nucleon interaction models. These newly developed models, denoted as Illinois models[31], incorporate the Fujita-Miyazawa and dispersive terms discussed above, but include in addition multipion exchange terms involving excitation of one or two Δ's, so-called pion-ring diagrams, as well as the terms arising from S-wave pion rescattering, required by chiral symmetry. A total of four parameters appear in these NNN interaction models, and GFMC calculations show that these can be adjusted to provide an excellent description of the low-lying spectra of systems with up to 10 nucleons.

Electro-weak currents

In the conventional approach, the nuclear electro-weak current operators are expressed in terms of one-body terms associated with the individual protons

14

and neutrons, and many-body terms modeled via pion- and heavier-meson-exchange mechanisms. It should be realized that these meson-exchange current (MEC) operators arise, as does the nucleon-nucleon interaction itself, as a consequence of the elimination of the mesonic degrees of freedom from the nuclear state vector. Clearly, such an approach is justified only at energies below the threshold for meson (specifically, pion) production, since above this threshold these non-nucleonic degrees of freedom have to be explicitly included in the state vector.

Electromagnetic current and charge operators

Two-body electromagnetic (and weak) current operators have conventionally been derived as the non-relativistic limit of Feynman diagrams, in which the meson-baryon couplings have been obtained either from effective chiral Lagrangians[59] or from semi-empirical models for the off-shell pion-nucleon amplitude[60]. These methods of constructing effective current operators, however, do not address the problem of how to model the composite structure of the hadrons in the phenomenological meson-baryon vertices. This structure is often parameterized in terms of form factors. For the electromagnetic case, however, gauge invariance actually puts constraints on these form factors by linking the divergence of the two-body currents to the commutator of the charge operator with the nucleon-nucleon interaction. The latter contains form factors too, but these are determined phenomenologically by fitting nucleon-nucleon data. Thus the continuity equation reduces the model dependence of the two-body electromagnetic currents by relating them to the form of the interaction. This point of view has been emphasized by Riska and collaborators[61]. The resulting currents are determined by the NN interaction, and contain no free parameters–they can therefore be viewed as model independent. There are, however, additional currents which, being purely transverse, are not constrained by the continuity equation, such as those associated with Δ-excitation or $\rho\pi$ transition couplings–the so-called model-dependent currents. The associated contributions are rather sensitive to the (poorly known) values for the coupling constants and short-range cutoffs, but fortunately are found be relatively small with respect to those of the model-independent currents[62].

Several uncertainties arise when considering the two-body charge operator, in contrast to the two-body current operator. While the main parts of the latter are linked to the form of the nucleon-nucleon interaction through the continuity equation, the most important two-body charge operators are model dependent and may be viewed as relativistic corrections. They fall into two classes. The first class includes those effective operators that represent non-nucleonic de-

15

grees of freedom, such as nucleon-antinucleon pairs or nucleon-resonances, and which arise when these degrees of freedom are eliminated from the state vector. To the second class belong those dynamical exchange charge effects that would appear even in a description explicitly including non-nucleonic excitations in the state vector, such as the $\rho\pi\gamma$ transition coupling. The proper forms of the former operators depend on the method of eliminating the non-nucleonic degrees of freedom. There are nevertheless rather clear indications for the relevance of two-body charge operators from the failure of calculations based on the one-body operator in predicting the charge form factors of the three- and four-nucleon systems [63,62], and deuteron tensor polarization observable [64]. Indeed, calculations including these two-body charge operators provide an excellent description of elastic and inelastic form factors of nuclei with $A \le 6$ [65].

The success of the present picture based on non-relativistic wave functions and a charge operator including the leading relativistic corrections should be stressed. It suggests, in particular, that the present model for the two-body charge operator is better than one *a priori* should expect. These operators fall into the class of relativistic corrections. Thus, evaluating their matrix elements with non-relativistic wave functions represents only the first approximation to a systematic reduction. A consistent treatment of these relativistic effects would require, for example, inclusion of the boost corrections on the nuclear wave functions. Yet, the excellent agreement between the calculated and measured charge form factors suggests that these corrections may be negligible in the q-range explored so far.

Weak current operators

The weak vector current and charge are constructed from the corresponding (isovector) electromagnetic terms, in accordance with the conserved-vector-current hypothesis, and thus have model-independent and model-dependent components, as discussed above.

The leading two-body terms in the axial current, in contrast to the case of the weak vector (or electromagnetic) current, are those due to Δ excitation, while the leading axial charge operator is the the long-range pion exchange term, required by low-energy theorems and PCAC. The largest model dependence is in the weak axial current. The $N\Delta$ axial coupling constant g_A^* is not well known. In the quark model, it is related to the axial coupling constant of the nucleon, and this value has often been used in the past to study Δ-induced axial current contributions to weak transitions. However, given the uncertainties inherent to quark-model predictions, a more reliable estimate for g_A^* is obtained by determining its value phenomenologically. It is well established

16

by now [66,67] that the one-body axial current leads to a $\simeq 4\%$ underprediction of the measured Gamow-Teller marix element in triutium β-decay. This small 4% discrepancy can then be used to determine g_A^*. While this procedure is inherently model dependent, its actual model dependence has in fact been shown to be very weak. The resulting axial current leads to predictions for the weak transitions in the $A =6$–7 nuclei, which are in excellent agreement with the experimental data [68].

Conventional and EFT aproaches

The EFT approach holds the promise of providing a a unified description of πN, NN, and NNN interactions and scattering, and indeed has been successfully applied to study low momentum πN processes. However, in the conventional approach, low momentum pions do not play a significant role in explaining nuclear binding and structure, since they couple only weakly to nucleons. The pion-exchange interaction provides $\simeq 75\%$ of the total two-body interaction energy, and most of its contribution comes from pions with momenta between 1.5 and 5 fm^{-1}. It also produces short-range structures of subfemtometer dimensions, as discussed above. Thus, the challenge for EFT is to push its applicability to pion momenta of up to 5 fm^{-1} for a realistic, quantitative study of nuclear properties, such as, for example, the deuteron tensor polarization. On the other hand, EFT can provide guidance to the conventional approach in the construction of more theoretically justified models for interactions and currents.

3 Experiment

Recent and new experimental results on studies of few-body nuclei indicate the existence of serious discrepancies between theory and experiment. The contributions to this working group meeting showed, for example, that whereas the Juelich meson exchange model correctly predicts the spin correlation coefficients and partial waves for the $pp \to pn\pi^+$ reaction at 375 MeV, it fails for the $pp \to pp\pi^0$ once P_s and P_p transitions become important.

One of the outstanding puzzles in few-body nuclear physics continues to be the so-called A_y puzzle, observed in the case of the three body system. Both n-d and p-d scattering data indicate a 30–40% discrepancy with theory. However, in this meeting we have seen preliminary reports [20] of new effective field theory calculations which appear to give much better agreement with the data. These results have to be carefully studied to understand the origin of this apparent agreement before any conclusions can be drawn. It is however, a very interesting and exciting result. There are also unresolved discrepancies

17

between theory and experiment in the case of radiative capture reactions of the $p + d$ system. In this case, potential model calculations fail to predict the amount of p-wave splitting observed in the experiments.

The four-body problem is in much worse shape. Both cross sections and spin observables in the $nT \rightarrow nT$, $dd \rightarrow dd$ and $dd \rightarrow pT$ reactions show large unexplained disagreements between theory and experiment. Besides this, an A_y discrepancy in p-^{3}He elastic scattering of almost a *factor of 2* exists at low energy (below 10 MeV). And the tensor observables in $dd \rightarrow dd$ and $dd \rightarrow p^3$H show deviations between theory and experiment which increase as the energy rises from 30 keV to 6 MeV. Even the $d + d$ radiative capture reaction cross section below 80 keV, which has been shown experimentally to proceed by p-wave capture at least 50% of the time, remains unexplained.

It is clearly important to perform precision measurements which test the predictions of few body theory. A preliminary study of deuterium was recently performed using the HIGS γ-ray beam [69] at an energy of 3.58 MeV [70]. The 100% linearly polarized beam was incident upon a deuterated liquid-scintillator target. Recoil signals from the target were used to generate a TOF spectrum. Four neutron detectors were placed in the up-down-left and right positions, and pulse-shape-discrimination was used to further reduce backgrounds. The result of these measurements at 150° led to an M1 contribution at 3.58 MeV of 9.2(1.8)%, in good agreement with the predictions of both potential model theory [71], which predicts an M1 contribution at this energy of 7.3%, and recent effective field theory calculations [72], which predicts an M1 contribution at 3.58 MeV of 7.85%. A plot of the theoretical prediction for the cross section, as well as the E1 and M1 components is presented in Fig. 1, along with the present experimental result. Note that the theoretical value of the total cross section was used in obtaining the experimental result shown in the figure.

The Gerasimov-Drell-Hearn Sum Rule in deuterium and ^{3}He is providing a new challenge to experimentalists and theorists. The GDH sum rule connects the helicity structure of the photo-absorption cross section to the anomalous magnetic moment of the nuclear target. It is derived using Lorentz and gauge invariance, crossing symmetry, causality and unitarity of the forward Compton scattering amplitude, and is explicitly given by

$$I_T = \int_{\omega_{\mathrm{th}}}^{\infty} d\omega \frac{\sigma_P(\omega) - \sigma_A(\omega)}{\omega} = 4\pi^2 \alpha s_T \left(\frac{\kappa_T}{m_T} \right)^2 , \qquad (1)$$

where σ_P and σ_A are the cross sections for absorption of polarized photons of energy ω and helicities parallel and antiparallel to the target spin s_T (in its maximum state), ω_{th} is the threshold photon energy for inelastic processes, α is the fine-structure constant, and m_T and κ_T are the target mass and anomalous
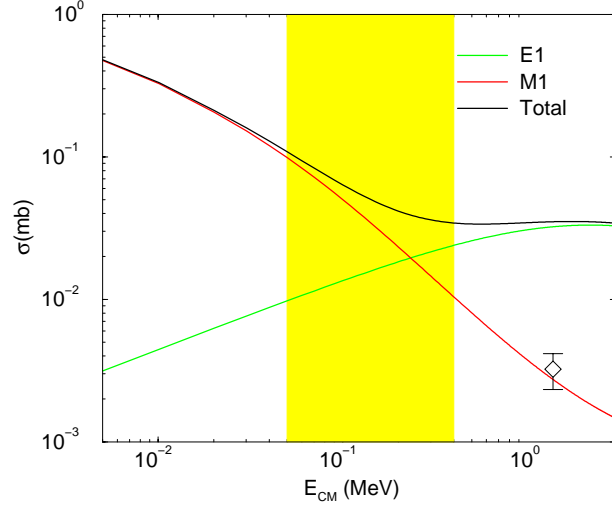
Figure 1: The theoretical total cross section [72] for the n-p capture reaction is shown along with the M1 and the E1 components. The previously measured cross-section data point is also shown, along with the present (HIGS 99) result for the M1 component at $E_\gamma = 3.58$ MeV.

magnetic moment, respectively [73,74].

Using the accepted values of the anomalous magnetic moments, we find that the values of the sum rule values for the proton, neutron and deuteron are: p: 204 μb, n: 232 μb, and d: 0.6 μb.

The GDH integral for the deuteron differs from that of the nucleons in that the lower limit in this case is the threshold for photo-disintegration (2.2 MeV), whereas it is photo-pion threshold in the case of the nucleons. The integral for the deuteron can be separated into two pieces by first integrating from photo-disintegration threshold up to pion threshold, and then integrating from pion threshold to infinity. If we (naively) assume that the part above pion threshold is simply the sum of the integrals for the proton and the neutron, we obtain 436 μb. This implies that the integral for the deuteron from photo-disintegration threshold up to pion threshold should have the value of -436 μb.

$$\text{i.e.} : \int_{2.2\text{MeV}}^{\omega_\pi} d\omega \frac{\sigma_P(\omega) - \sigma_A(\omega)}{\omega} = -436 \ \mu\text{b}. \tag{2}$$

The integrand of the GDH sum rule can be written in terms of the contributing transition matrix elements. In the photo-disintegration threshold

region these are expected to be only the E1 and M1 matrix elements. There are 4 p-wave (E1) terms, one of which is $\Delta S=1$, and can therefore be ignored. If the other three reduced matrix elements are considered to be j-independent, as expected at these energies, their contribution to the GDH integrand vanishes. There are two M1 matrix elements. The one having S=1 and L=0 is expected to vanish, since it will be orthogonal to the ground state of the deuteron. Hence, we are left with just one matrix element corresponding to having S=0, L=0 and J=0. Since the total M1 cross section will be proportional to the square of this matrix element, we can write a relationship between the total M1 cross section and the integrand (i.e. $\sigma_P(\omega) - \sigma_A(\omega)$) of the GDH sum rule. The result of our measured value of the M1 cross section leads to a value of $\sigma_P(\omega) - \sigma_A(\omega)$ at 3.58 MeV of $-529(160)$ μb. This result is shown in Fig. 2 along with the theoretical prediction of Arenhoevel *et al.* [71]. Although indirect, this is the first experimental result for the GDH integrand in the vicinity of the photodisintegration threshold. As seen in Fig. 2, a major portion of the GDH sum rule integrand for the deuteron lies in the region below E_x=3.0 MeV, arising from the $^1S_0$ resonance in the deuteron.
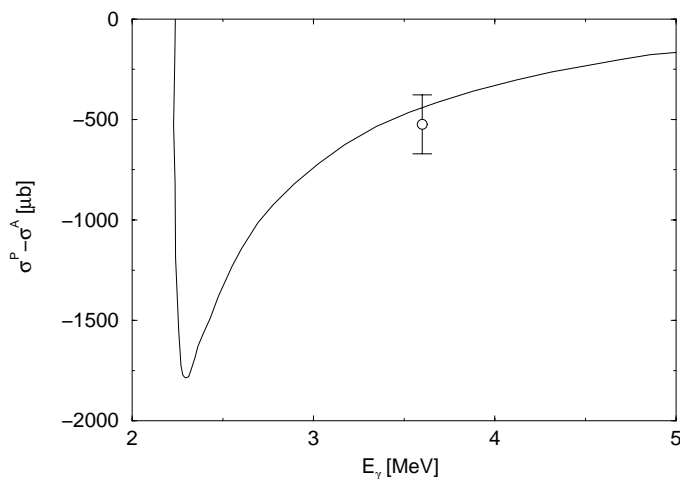

Figure 2: The theoretical prediction for $\sigma_P - \sigma_A$ [71] as a function of E_γ for the deuteron along with the preliminary experimental results deduced from our experiments (see text).

In ^{3}He, the GDH sum rule is $I_{^3\mathrm{He}} = 498$ μb, using the experimental value $\kappa_{^3\mathrm{He}} = -8.366$. It is again useful to divide the integral into the part up to pion threshold, and the part above this threshold. For the part above pion threshold, the ^{3}He nucleus should have roughly the same strength as the neutron, i.e.

$\simeq 230\ \mu$b. Such an expectation is based on the fact that the ^{3}He ground state consists predominantly of a spherically symmetric S-wave component, in which the proton spin projections are opposite and the net polarization is therefore due entirely to the neutron. Ignoring corrections to this naive estimate, it is expected that the ω-region from the photodisintegration threshold ($\omega_{\text{th}} = 5.4949$ MeV) up to the pion threshold should contribute about 266 μb to the ^{3}He GDH sum rule.

To date, the studies of the GDH sum rule for the case of ^{3}He have been limited to the region at and above photodisintegration threshold. In this case, we have not made a direct measurement of the σ_P and σ_A photo-absorption cross sections to determine the contribution to $I(\overline{\omega})$, instead we have determined its value from measurements of the cross sections, vector and tensor analyzing powers for the radiative capture reactions $D(p,\gamma)^3$He and $p(d,\gamma)^3$He [75]. These measurements allow the determination of the complex reduced matrix elements (RMEs) of these reactions. This has been performed at TUNL for proton and deuteron incident energies in the range 0–80 keV, corresponding to values $\omega_{\text{th}} \leq \omega \leq 5.548$ MeV [75].

In the energy region under consideration here (pd relative energies less than 53 keV), there are only six dominant RMEs corresponding to magnetic and electric dipole transitions (M1 and E1, respectively) resulting in emission of pd pairs in relative S- and P-wave states. Thus, ignoring the contribution of higher order multipoles, we find [76]:

$$
\begin{aligned}
\Delta\sigma &\equiv \sigma_P - \sigma_A \\
&= \frac{16\pi^2\alpha\mu p}{\omega}\left[-|s_2|^2 + \frac{|s_4|^2}{2}\right.\\
&\quad \left. -|p_2|^2 + \frac{|p_4|^2}{2} - |q_2|^2 + \frac{|q_4|^2}{2}\right],
\end{aligned}
\tag{3}
$$

where for ease of presentation we have introduced the notation $s_{2J+1} \equiv M_1^{0JJ}$, $p_{2J+1} \equiv E_1^{1\frac{1}{2}J}$, and $q_{2J+1} \equiv E_1^{1\frac{3}{2}J}$ for J=1/2 and 3/2 (the superscripts in X_ℓ^{LSJ}, $X = M, E$, refer respectively to the quantum numbers LSJ defined above). The energy dependence of the RMEs and $\Delta\sigma$ is understood.

The data of this experiment were obtained using frozen H$_2$O and D$_2$O targets and large HPGe detectors. This, as discussed in Schmid $et\ al.$ [77], allowed us to obtain the cross section and analyzing powers as a function of energy. This was accomplished by de-convoluting the full-energy peak in the spectrum, which was broadened when the 80 keV proton beam, for example, stopped in the ice target. Of course it was the high resolution (about 4.2 keV)

$\overline{\omega}$ (MeV)	$I(\overline{\omega})$	FIT	IA	FULL
5.522	M1	-0.0524 ± 0.0077	-0.0016	-0.0485
5.522	E1 $S =1/2$	-0.0361 ± 0.0095	-0.0030	$+0.0027$
5.522	E1 $S =3/2$	-0.0026 ± 0.0007	-0.0050	-0.0001
5.522	Total	-0.0911 ± 0.0123	-0.0096	-0.0459
5.548	Total	-1.120 ± 0.218	-0.149	-0.435

Table 1: The contributions $I(\overline{\omega})$ (in nb) for two energies $\overline{\omega}$. In the third column, the values obtained from a fit of the experimental pd capture data are reported. The results of the theoretical calculations obtained with one-body only and both one- and two-body currents are listed in the fourth and fifth columns, labeled IA and FULL respectively. The lines denoted by M1, E1 $S=1/2$ and E1 $S=3/2$ report the partial contributions to $I(\overline{\omega}=5.522$ MeV) of the corresponding RMEs.

of the detector which made this possible.

The current data set are sufficient to determine the six contributing matrix elements and their five relative phases in an unconstrained fit. If we assume that the ratio of the doublet-to-quartet M1 strengths and the $J = 3/2$ to $1/2$ E1 strengths are equal to the values we obtained at $E_{\mathrm{c.m.}} = 26.6$ keV, we can perform the integral of Eq. (1). The results corresponding to integrating up to $\overline{\omega}_1 = 5.522$ MeV ($E_p = 40$ keV) or to $\overline{\omega}_2 = 5.548$ MeV ($E_p = 80$ keV) are presented in Table 1. While this is an insignificant (negative) contribution to the total strength expected below pion threshold, it is an interesting result which can be compared directly with the predictions of the three-body model calculations[78].

A detailed description of the theoretical calculations which provide the basis for a comparison and interpretation of the experimental capture results obtained above has been previously published[78]. With respect to this earlier reference, however, we note that in the present work the variational treatment of the pd continuum states has been improved. As a result, the present calculations are in better agreement than reported in 1996[78] with the many experimental capture data obtained below 80 keV. In particular, the discrepancy between the calculated and measured A_y observable has been reduced substantially.

The value of the GDH sum rule integral $I(\overline{\omega})$ predicted with inclusion of one-body only and both one- and two-body currents (columns labeled IA and FULL, respectively) are reported in Table 1 for $\overline{\omega}_1=5.522$ MeV and $\overline{\omega}_2=5.548$ MeV. Table 1 also lists the individual contributions to $I(\overline{\omega}_1)$ from the $-|s_2|^2 + |s_4|^2/2$, $-|p_2|^2 + |p_4|^2/2$, $-|q_2|^2 + |q_4|^2/2$ RME combinations (rows labeled M1, E1 $S=1/2$, and E1 $S=3/2$, respectively).

22

The total contribution to $I(\overline{\omega})$ is mostly due to M1 strength. While the results in the "full" calculation are in much better agreement with data than those in IA, a factor of two discrepancy persists between theory and experiment. This discrepancy is mostly due to the difference between the calculated and measured $S=1/2$ E1 strength, as the second row in Table 1 makes clear. The difference in the strengths of $|p_2|^2$ and $|p_4|^2/2$ observed in the experimental results is presently unaccounted for. Perhaps it is due to a spin-dependent 3-body force similar to that recently proposed to account for the so-called A_y problem[79]. Further theoretical work is needed here.

The three-body model calculations[78] allow for the evaluation of $\sigma_P - \sigma_A$ up to three-body breakup threshold. Preliminary results indicate that the value of the GDH integral (Eq.1), when computed up to this threshold, is about 1.2 μb, still a negligible contribution to the sum rule value. These calculations indicate that the contribution to the GDH sum in this region arises primarily from the difference between the two s=1/2 E1 matrix elements having j=1/2 and j=3/2, respectively. The M1 effects, which dominate the threshold region, are negligible in comparison to this.

Polarized capture data have been obtained at $E_{c.m.} = 2.0$ MeV, corresponding to E_x=7.5 MeV [80]. The capture matrix elements were extracted from these data using a technique, based on Watson's Theorem, which allowed for the use of the elastic scattering phase shifts as additional input. Two solutions were found: Set 1 and Set 2. Set 1 is physically preferred since it has equal singlet and doublet M1 amplitudes, similar to theory, whereas Set 2 has the doublet M1 strength set to zero. The amplitudes of Set 1 can be used to calculate $\sigma_P - \sigma_A$, which can be compared to the value predicted by theory. The result indicates an experimental value of $\sigma_P - \sigma_A = 0.0042$. This result arises mainly from the two s=1/2 E1 matrix elements, as predicted by theory. However, the theoretical value for $\sigma_P - \sigma_A$ at E_x=7.5 MeV is almost four times as large (0.016 mb), suggesting that the splitting of the two p-wave amplitudes is too large in the theory. However, the error in the experimental result (estimated to be about ± 0.03) makes any definite conclusion impossible at this time. These preliminary results clearly indicate the need for further study in the energy regime below three-body breakup threshold.

Polarized capture data have made it possible to determine the value of the integral which defines the GDH sum rule in the region just above threshold in ^{3}He. While the results indicate that an extremely tiny piece of the total sum-rule strength is located in this region, we have found, by direct comparison with theory, that this integral observable is very sensitive to the effects of two-body currents. The inclusion of these currents reduces the discrepancy between theory and experiment from a factor of 10 to a factor of 2. Further theoretical

23

progress is needed to understand the physical origin of the difference in the p-wave E1 RMEs responsible for the remaining discrepancy. This first glimpse of the GDH integral for ^{3}He, although insignificant to the Sum Rule value, demonstrates the new knowledge contained in this quantity and emphasizes the need for measurements at higher energies.

Clearly, future experimental studies should focus on precision measurements and should be done using polarized beams and polarized targets. These observables provide the sensitivities needed to test and evolve the theories. One of the new facilities described in this workshop[69], the new High-Intensity Gamma-Ray Source (HIGS) presently under construction at TUNL, should play a major role in these future studies. Circularly polarized beams will be available at HIGS in about two years. These will be used along with the TUNL frozen-spin polarized targets[81] to perform a direct measurement of the GDH sum-rule integral for the deuteron from 3-to-30 MeV. Circularly polarized beams and the TUNL solid polarized ^{3}He target[82] will be used to measure the 3-body photo-disintegration channel contribution to $\sigma_P - \sigma_A$ for energies from 8-to-50 MeV. This will consist of a measurement of $\sigma_P - \sigma_A$ for the ^{3}He$(\gamma, n)pp$ reaction at energies from 8-to-50 MeV. An incident flux of 10^7 γ/s indicates a neutron count rate of about 4000/hr at $90°$ at a γ energy of 14 MeV. This work should also begin in about 2 years.

The results of effective field theory calculations, as well as calculations based on two-body potentials derived using effective field theory, promise to provide new insights into the limitations of our present understanding of these systems - especially when combined with the precision polarized data we anticipate in the near future.

References

1. S. Weinberg, *Phys. Lett.* B **251**, 288 (1990); *Nucl. Phys.* B **363**, 3 (1991); *Phys. Lett.* B **295**, 114 (1992).
2. C. Ordóñez and U. van Kolck, *Phys. Lett.* B **291**, 459 (1992); C. Ordóñez, L. Ray and U. van Kolck, *Phys. Rev. Lett.* **72**, 1982 (1994); *Phys. Rev.* C **53**, 2086 (1996).
3. U. van Kolck, *Phys. Rev.* C **49**, 2932 (1994).
4. T.-S. Park, D.-P. Min, and M. Rho, *Phys. Rep.* **233**, 341 (1993); *Nucl. Phys.* A **596**, 515 (1996).
5. S.R. Beane, V. Bernard, T.-S.H. Lee, U.-G. Meißner, and U. van Kolck, *Nucl. Phys.* A **618**, 381 (1997).
6. D.B. Kaplan, M.J. Savage, and M.B. Wise, *Nucl. Phys.* B **478**, 629 (1996).
7. U. van Kolck, in *Proceedings of the Workshop on Chiral Dynamics 1997, Theory and Experiment*, ed. A. Bernstein, D. Drechsel, and T. Walcher (Springer-Verlag, 1998), `hep-ph/9711222`.
8. D.B. Kaplan, M.J. Savage, and M.B. Wise, *Phys. Lett.* B **424**, 390 (1998); *Nucl. Phys.* B **534**, 329 (1998).
9. J. Gegelia, `nucl-th/9802038`; `nucl-th/9805008 v2`.
10. U. van Kolck, in *Nuclear Physics with Effective Field Theory*, ed. R. Seki, U. van Kolck, and M.J. Savage (World Scientific, 1998); *Nucl. Phys.* A **645**, 273 (1999).
11. H.-W. Hammer, Contribution to this working group.
12. J.L. Friar, D. Hüber, H. Witala, and G.L. Payne, *Acta Phys. Polon.* B **31**, 749 (2000).
13. F. Gabbiani, Contribution to this working group.
14. M.J. Savage, Contribution to this working group.
15. J.-W. Chen, Contribution to this working group.
16. U. van Kolck, *Few-Body Syst. Suppl.* **9**, 444 (1995).
17. U. van Kolck, *Prog. Part. Nucl. Phys.* **43**, 337 (1999).
18. M.C.M. Rentmeester, R.G.E. Timmermans, J.L. Friar, and J.J. de Swart. *Phys. Rev. Lett.* **82**, 4992 (1999).
19. M. Robilotta, Contribution to this working group.
20. U.-G. Meißner, Contribution to this working group.
21. T. Mehen, Contribution to this working group.
22. H. Grießhammer, Contribution to this working group.
23. C. Hanhart, Contribution to this working group.
24. U. van Kolck, Contribution to this working group.
25. S.R. Beane, Contribution to this working group.

26. K. Kubodera, Contribution to this working group.
27. R. Schiavilla, `nucl-th/0010062`.
28. R.A. Malfliet and J.A. Tjon, *Nucl. Phys.* A **127**, 161 (1969).
29. C.R. Chen *et al.*, *Phys. Rev.* C **31**, 2266 (1985).
30. J. Carlson, *Nucl. Phys.* A **508**, 141c (1990).
31. S.C. Pieper *al.*, `nucl-th/0102004`
32. W. Glöckle *et al.*, *Phys. Rep.* **274**, 107 (1996).
33. A. Kievsky *et al.*, *Phys. Rev.* C **58**, 3085 (1998).
34. J.L. Friar, B.F. Gibson, and G.L. Payne, *Phys. Lett.* B **251**, 11 (1990).
35. J.L. Friar *et al.*, *Phys. Rev. Lett.* **66**, 1827 (1991).
36. M. Viviani, R. Schiavilla, and A. Kievsky, *Phys. Rev.* C **54**, 534 (1996).
37. M. Viviani *et al.*, *Phys. Rev.* C **61**, 064001 (2000).
38. R. Schiavilla *et al.*, *Phys. Rev.* C **45**, 2628 (1992).
39. A. Arriaga, V.R. Pandharipande, and R. Schiavilla, *Phys. Rev.* C **43**, 983 (1991).
40. J. Carlson and R. Schiavilla, *Rev. Mod. Phys.* **70**, 743 (1998).
41. R. Machleidt, *Phys. Rev.* C **63**, 024001 (2001).
42. V.G.J. Stoks *et al.*, *Phys. Rev.* C **49**, 2950 (1994).
43. R.B. Wiringa, V.G.J. Stoks, and R. Schiavilla, *Phys. Rev.* C **51**, 38 1995).
44. J.L. Friar, *Ann. Phys. (N.Y.)* **104**, 380 (1977).
45. J.L. Forest, *Phys. Rev.* C **61**, 034007 (2000).
46. S.A. Coon and J.L. Friar, *Phys. Rev.* C **34**, 1060 1986).
47. R. Schiavilla, `nucl-th/0010062`.
48. J.L. Forest *et al.*, *Phys. Rev.* C **54**, 646 (1996).
49. D. Abbott *et al.*, *Phys. Rev. Lett.* **82**, 1379 (1999).
50. J.S. Levinger and H.A. Bethe, *Phys. Rev.* **78**, 115 (1950).
51. A. Akmal and V.R. Pandharipande, *Phys. Rev.* C **56**, 2261 (1997).
52. J. Fujita and H. Miyazawa, *Prog. Theor. Phys.* **17**, 360 (1957).
53. A. Picklesimer, R.A. Rice, and R. Brandenburg, *Phys. Rev.* C **45**, 2624 (1992).
54. P.U. Sauer, *Nucl. Phys.* A **543**, 291c (1992).
55. S.A. Coon *et al.*, *Nucl. Phys.* A **317**, 242 (1979).
56. M.R. Robilotta, *Few-Body Syst. Suppl.* **2**, 35 (1987).
57. B.S. Pudliner *et al.*, *Phys. Rev. Lett.* **74**, 4396 (1995).
58. S.C. Pieper and R.B. Wiringa, `nucl-th/0103005`.
59. D.O. Riska, *Prog. Part. Nucl. Phys.* **11**, 199 (1984).
60. M. Chemtob and M. Rho, *Nucl. Phys.* A **163**, 1 (1971); **212**, 628(E).
61. D.O. Riska, *Phys. Rep.* **181**, 207 (1989).
62. L.E. Marcucci, D.O. Riska, and R. Schiavilla, *Phys. Rev.* C **58**, 3069

(1998).

63. R. Schiavilla, V.R. Pandharipande, and D.O. Riska, *Phys. Rev.* C **41**, 309 (1990).
64. R. Schiavilla and D.O. Riska, *Phys. Rev.* C **43**, 437 (1991).
65. R.B. Wiringa and R. Schiavilla, *Phys. Rev. Lett.* **81**, 4317 (1998).
66. R. Schiavilla *et al.*, *Phys. Rev.* C **58**, 1263 (1998).
67. L.E. Marcucci *et al.*, *Phys. Rev.* C **63**, 015801 (2001).
68. R. Schiavilla and R.B. Wiringa, unpublished.
69. H.R. Weller, Contribution to this working group.
70. E.C. Schreiber *et al.*, *Phys. Rev.* C **61**, 061604(R) (2000).
71. H. Arenhoevel, G. Kress, R. Schmidt, and P. Wilhelm, *Nucl. Phys.* A **631**, 612c (1998).
72. J.W. Chen and M.J. Savage, *Phys. Rev.* C **60**, 065205 (1999).
73. S.B. Gerasimov, *Sov. J. Nucl. Phys.* **2**, 430 (1966).
74. S.D. Drell and A.C. Hearn, *Phys. Rev. Lett.* **16**, 908 (1996).
75. E.A. Wulf *et al.*, *Phys. Rev.* C **61**, 061601(R) (1999).
76. H.R. Weller *et al.*, *Atomic Data and Nuclear Data Tables* **58**, 219 (1994).
77. G.J. Schmid *et al.*, *Phys. Rev. Lett.* **76**, 3088 (1996); G.J. Schmid *et al.*, *Phys. Rev.* C **56**, 2565 (1997).
78. M. Viviani, R. Schiavilla, and A. Kievsky, *Phys. Rev.* C **54**, 534 (1996).
79. D. Hüber and J.L. Friar, *Phys. Rev.* C **58**, 674 (1998).
80. M.K. Smith and L.D. Knutson, *Phys. Rev. Lett.* **82**, 4591 (1999).
81. D. Haase, NCSU and TUNL, private comm. (2000).
82. C.D. Keith *et al.*, *Nuclear Inst. and Methods in Phys. Res.* A **357**, 34 (1995).